

Numerical study of steel sandwich plates with RPF and VR cores materials under free air blast loads

Mohamed Rashad^{2a} and T.Y. Yang^{*1,2}

¹ International Joint Research Laboratory of Earthquake Engineering, Tongji University, Shanghai, China

² Department of Civil Engineering, University of British Columbia, Vancouver, Canada

(Received July 9, 2017, Revised November 14, 2017, Accepted December 3, 2017)

Abstract. One of the most important design criteria in military tunnels and armoured doors is to resist the blast loads with minimum structural weight. This can be achieved by using steel sandwich panels. In this paper, the nonlinear behaviour of steel sandwich panels, with different core materials: (1) Hollow (no core material); (2) Rigid Polyurethane Foam (RPF); and (3) Vulcanized Rubber (VR) under free air blast loads, was investigated using detailed 3D nonlinear finite element models in Ansys Autodyn. The accuracy of the finite element model proposed was verified using available experimental test data of a similar steel sandwich panel tested. The results show the developed finite element model can be reliably used to simulate the nonlinear behaviour of the steel sandwich panels under free air blast loads. The verified finite element model was used to examine the different parameters of the steel sandwich panel with different core materials. The result shows that the sandwich panel with RPF core material is more efficient than the VR sandwich panel followed by the Hollow sandwich panels. The average maximum displacement of RPF sandwich panel under different ranges of TNT charge (1 kg to 10 kg at a standoff distance of 1 m) is 49% and 53% less than the VR and Hollow sandwich panels, respectively. Detailed empirical design equations were provided to quantify the maximum deformation of the steel sandwich panels with different core materials and core thickness under a different range of blast loads. The developed equations can be used as a guide for engineer to design steel sandwich panels with RPF and VR core material under a different range of free air blast loads.

Keywords: 3D nonlinear finite element analysis; rigid polyurethane foam (RPF); vulcanized rubber (VR); free air blast loads

1. Introduction

Steel sandwich panels can be used as the protection layers for blast resisting doors, as it possesses high stiffness to weight ratio and has outstanding energy absorption capabilities (Vinson 2001). Experimental and analytical investigations of steel sandwich panels, with either honeycomb or metal foam cores under free air blast loads, have been investigated in the past (Zhu 2008, Nurick *et al.* 2009, Lee and O'Toole 2004, Yen *et al.* 2005, Xia *et al.* 2016, Fayad 2009, Mazek 2014). These steel sandwich panels have demonstrated high energy dissipating capacity. In this paper, an innovative steel sandwich panels with different core materials: (1) rigid polyurethane foam (RPF); and (2) Vulcanized Rubber (VR), under free air blast loads was investigated. The proposed steel sandwich panel with RPF and VR are significantly lighter than the steel sandwich panels with either honeycomb or metal foam cores. RPF has been used by different researchers (Woodfin *et al.* 1998, Mostafa *et al.* 2010a, b, Woodfin 2000, Sheikh and Li 2007) to absorb the impact from the blast loads. In these studies, hyperelastic RPF was used as a single

protective layer or as a retrofitting layer instead of the core material for the blast load. Although retrofitting steel sandwich panels with RPF or Polyurea layer has been shown to be able to absorb a considerable amount of explosion energy, RPF is very sensitive to the high temperature emitted from the explosion load (Rashad 2013, Mazek and Mostafa 2014, Mazek and Wahab 2015, Ha *et al.* 2011). As a result, the strength and the energy absorption capability of the sandwich panel could be significantly compromised. In this study, a high-density RPF was used as the core material for the steel sandwich panels. This way, the RPF was protected by the steel sandwich plates on the outsides. Hence, it can be more efficiently used to dissipate the blast energy.

Similar to RPF, VR has been used in many structural applications. Chen *et al.* (2009) and Xiao *et al.* (2014) have used VR to reduce the high-frequency vibration and blast resistance for ships. Li *et al.* (2016) showed that high damping rubber interlayer could enhance the antiknock behavior of armored doors when subjected to blast loads. Wang and Ko (2015) show that by adding VR layer to composite steel connector can improve the energy dissipation capacity under different quasi-static and dynamic loading conditions. In the present study, a VR layer was used as the core material within the sandwich panel which was protected from high temperature by the steel cover plates.

*Corresponding author, Executive Director,
E-mail: yang@ilee-tj.com

^a Ph.D. Student, E-mail: mohamed.rashad@civil.ubc.ca

To simulate the nonlinear behavior of steel sandwich panels with Hollow, RPF and VR core materials, a detailed numerical model was developed using Ansys Autodyn (Ansys 2007). Ansys Autodyn is a commercially available software designed to solve the nonlinear behavior of structure under fast impact loads. To ensure the algorithm converges, an explicit numerical algorithm, known as “hydrocodes” was used in this study. The “hydrocodes” solve the momentum and energy conservation of the system simultaneously. The developed finite element model was verified using available experimental data. The result shows the proposed finite element model can be used to simulate the nonlinear dynamic response of the steel sandwich panels well.

Once the finite element model has been verified, 36 variations of the finite element model were developed to systematically examine the nonlinear behaviour of the steel sandwich panel under free air blast loads. The model consists of 3 types of lightweight sandwich panels with 4 different core thicknesses (5, 10, 15 and 20 cm) and subjected to 3 levels of explosion pressures (1, 5 and 10 kg TNT charges at a standoff distance (SOD) of 1 m). Based on the results of the parameter study, robust design equations were developed. The developed design equation can be used efficiently by engineers to size the steel sandwich panel with different core (RPF or VR) material under different blast load applications.

2. Development and validation of the finite element model

2.1 Modelling of the blast pressure

Table 1 Material data of air and TNT used in the model

Material	Air	TNT	TNT (Ideal)
Equation of state	Ideal gas	JWL	Ideal gas
Initial conduction	$\rho = 1.225 \times 10^{-3} \text{ g/cm}^3$	Default	From detonation
Density	$1.225 \times 10^{-3} \text{ g/cm}^3$	Library data	$1.0 \times 10^{-3} \text{ g/cm}^3$
Ideal gas constant	$\gamma = 1.4$	Standard	$\gamma = 1.35$
Reference energy	$2.068 \times 10^5 \text{ } \mu\text{J/mg}$		Model/remap data

To properly model the behaviour of the TNT explosion, a numerical model in Ansys Autodyn was developed. In the numerical model, the air was modeled using the Hydro model, which has no strength and the TNT was modeled using the Jone Wilkins-Lee (JWL) model (Ansys 2007). JWL model was used because it can simulate the rapid expansion of TNT when detonated. After the TNT was detonated, the pressure created by the TNT detonation was modeled using ideal gas EOS (equation of state). Ideal gas EOS is widely used by blast researchers because it is simple to use and yet it can simulate the pressure created by the explosion very well. Table 1 shows the property of the air and TNT used in this study. Eq. (1) shows the pressure model of the ideal gas when the TNT exploded.

$$P_{EOS} = A \left(1 - \frac{w}{R_1 V} \right) e^{-R_1 V} + B \left(1 - \frac{w}{R_2 V} \right) e^{-R_2 V} + w \frac{E}{V} \quad (1)$$

where A , B , R_1 , R_2 , and w are the JWL parameters, presented in Table 2, that are used to model the air and TNT material; $V = \frac{\rho_{SOL}}{\rho}$, where ρ and ρ_{SOL} are the current and solid density of the explosive, respectively; $E = \rho_{SOL} e_{int}$ = the internal energy per unit volume of the explosive, where e_{int} is the current internal energy per unit mass;

Once the 2D pressure has been calculated (using Eq. (1)), the pressure is then mapped into a 3D finite element model, as shown in Fig. 1. This procedure is commonly used by blast engineers to decrease the computational effort needed to simulate the explosion process in a 3D finite element model.

In the 3D model, Euler-FCT (Flux corrected Transport) formulation was used to solve the nonlinear dynamic response of the air. Euler-FCT is generally designed to

Table 2 Summary of the parameters used to model TNT

JWL parameter	TNT
A (GPa)	373.75
B (GPa)	3.747
R1	4.15
R2	0.90
w	0.35

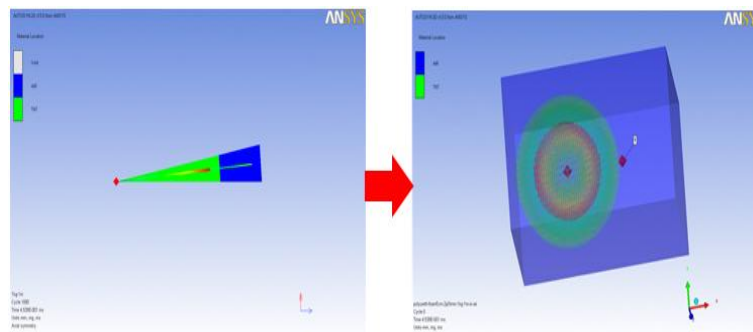


Fig. 1 Remapping of the TNT charge from 2D and 3D



Fig. 2 Structural steel frame for explosion field tests and sensor reading of 1 kg TNT at 1 m

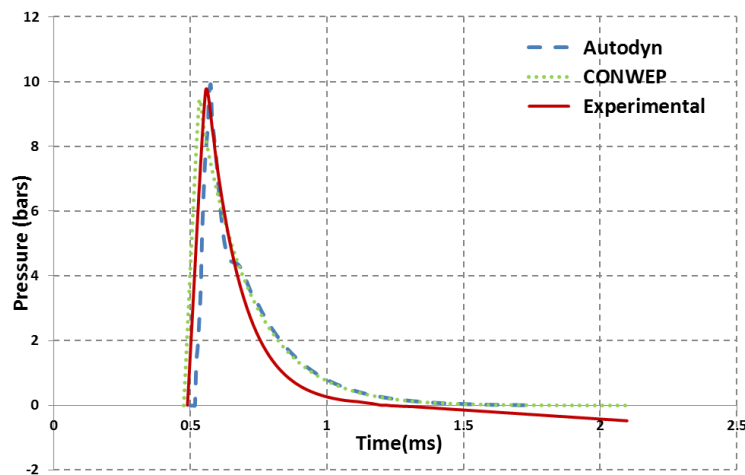


Fig. 3 Pressure time history of 1 kg TNT exploded at SOF of 1 m

solve gas dynamic problems including large deformations and/or fluid flow. Euler-FCT can model the air where there is no grid distortion in this element. This means that there is no change in size and shape of the element during the analysis. In this case, the time step (Δt) controlled by this element type will be constant throughout the analysis. The boundary condition of the surrounding air is chosen as flow out at the six faces of the air block.

The pressure generated from the finite element model was verified using a simple experimental test and compared with the empirical value presented in the TM5 document (TM 5-885-1 1986). Fig. 2(a) shows the test rig used to verify the blast pressure. In this test, a 1 kg TNT was set off at the center of the steel frame. Fig. 2(b) shows the sensor used to measure the pressure time history. Fig. 3 shows the comparison of the pressure time history between the numerical simulation, empirical calculation, and experimental data. The result shows excellent match between the experimental testing and finite element modeling. In addition, the peak overpressure was compared with the CONWEP (Hyde 1991) program. Table 3 shows the comparison of the peak overpressure values. The result shows that the finite element model is within 2.5% and 3.1% of the experimental and empirical solutions, respectively. This shows the proposed model can be used to effectively model the pressure generated by the TNT blast.

Table 3 Comparison of the peak overpressure

Empirical equations	Experimental simulation	Numerical simulation
9.35 bar	9.65 bar	9.91 bar

2.2 Modelling of steel sandwich panels

Fig. 4 shows the finite element model developed for this study. The steel plates were modeled using shell elements. Shell element permits the translation and rotation in three directions, which can be used to model both membrane (in-plane) and the plate (out-of-plane) members. Standard Lagrange formulation was used to model the shell elements. The Johnson and Cook strength model (Johnson and Cook 1983) was used to model the steel material which is ideal for materials subjected to large strains, high strain rates, and high temperatures. The Johnson and Cook constitutive model is presented in Eq. (2) (Ansys 2007).

$$Y = [A + B\varepsilon_p^n][1 + C \ln \dot{\varepsilon}_p][1 - T_H^w] \quad (2)$$

Where A is the yield stress; B is the strain hardening constant; ε_p is the effective plastic strain; n is the strain hardening exponent; C is the strain rate constant; $\dot{\varepsilon}_p$ is the

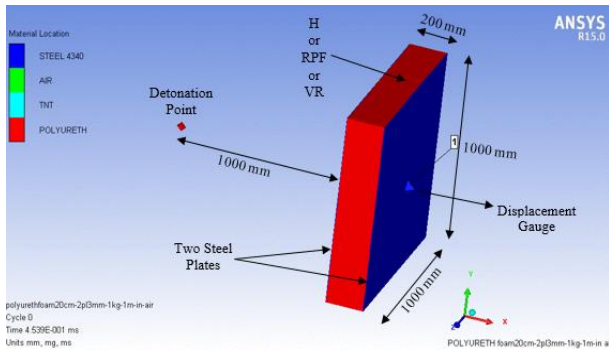


Fig. 4 The proposed finite element model

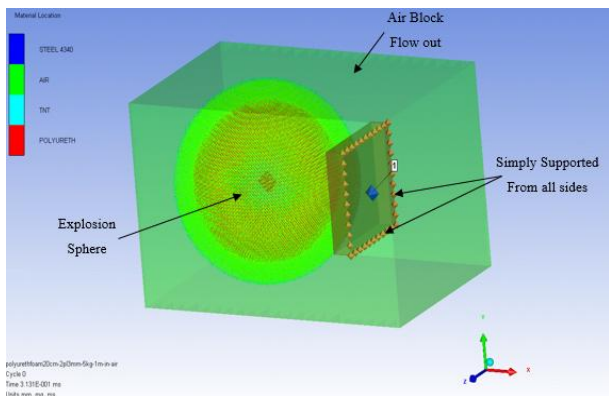
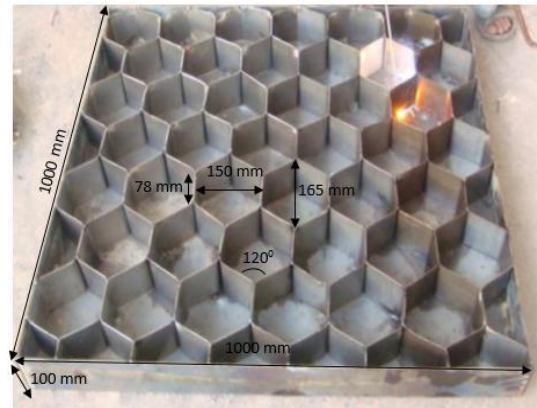
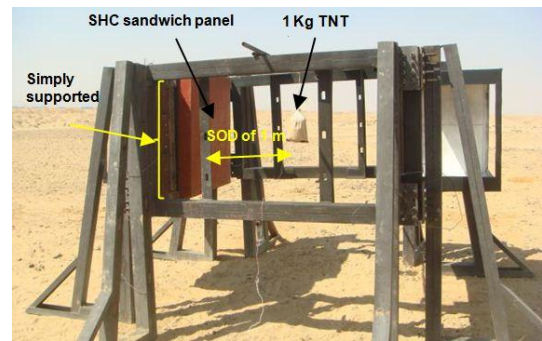


Fig. 5 Boundary conditions of the sandwich panel and the air media which include the explosion sphere



(a) Dimensions and core configuration



(b) Test rig

Fig. 6 SHC sandwich panel, and the used test rig (Mazek and Mostafa 2013)

normalized effective plastic strain rate; T_H is the homologous temperature given by $T_H = (T - T_{room}) / (T_{melt} - T_{room})$; w is the thermal softening exponent.

The first set of brackets gives the yield stress as a function of strain at room temperature and a strain rate of 1 s^{-1} , which is the default reference strain rate, accounting for the effect of strain hardening. The second set of brackets modifies the yield stress based on the strain rate. The third bracket accounts for thermal softening causing the yield stress to become zero when the temperature reaches the melting point.

Fig. 5 shows the boundary conditions of the proposed finite element model for the sandwich panel and the air media, which included the explosion sphere as presented in Fig. 1. The finite element model was assumed to be simply supported from the four sides.

To verify the analytical model, a steel sandwich panel with steel hexagonal core (SHC) was modeled and verified against available experimental data. Fig. 6(a) shows the SHC sandwich panel presented in this study. In this study, the cover steel plates have a dimension $1000 \text{ mm} \times 1000 \text{ mm}$ and a thickness of 6 mm. These two steel plates were separated by hexagonal honeycomb steel core layer with a depth of 100 mm. The thickness of each hexagonal honeycomb unit is 1 mm. The interior perpendicular dimension of each honeycomb unit is $165 \text{ mm} \times 150 \text{ mm}$. Fig. 6(a) shows the dimensions and the core configuration of the SHC. The SHC sandwich panel was subjected to a free air blast load of 1 kg of TNT detonated at a standoff

Table 4 Mechanical properties of the steel used in SHC sandwich panel

Material	Steel
Reference density	7.83 g/cm^3
Yield stress	$3.5 \times 10^5 \text{ KPa}$
Shear modulus	$8.18 \times 10^7 \text{ KPa}$
Bulk modulus	$1.59 \times 10^8 \text{ KPa}$
Poisson ratio	0.3

distance of 1 m. Fig. 6(b) shows the test rig which was used for the free air blast tests. Table 4 shows the mechanical properties of the steel used to model the SHC (Mazek and Mostafa 2013).

The maximum displacement of the SHC panel from the experimental test was compared with the finite element simulation shown in Table. 5. The result shows the maximum deformation of the sandwich panel estimated

Table 5 Comparison of the maximum displacement value of the SHC sandwich panel between experimental and numerical simulations

Sandwich panel	Experimental	Numerical	Percent difference
SHC	4.40 mm	4.20 mm	4.5 %

Table 6 Mechanical properties of the RPF used in this study

Material	RPF
Reference density	1.265 g/cm ³
Principal tensile failure stress	3.45 × 10 ⁴ KPa
Shear modulus	5 × 10 ³ KPa
Bulk modulus	20 × 10 ⁵ KPa

Table 7 Mechanical properties and parameters of the VR used in this study

Material	VR
Reference density	1.0 g/cm ³
Mu1, Mu2, Mu3	(618.03, 1.18, -9.81) KPa
Alpha1, Alpha2, Alpha3	1.3, 5, -2

from the proposed finite element model is within 5% of the experimental data. This shows the proposed model can be used to reliably simulate the deformation of the steel sandwich panels.

2.3 Modelling of steel Sandwich panels with PRF and VR core materials

After the finite element modeling of the steel sandwich panels with SHC has been verified, the same modeling approach was used to model the response of steel sandwich panels with RPF and VR core materials. The proposed sandwich panel consists of two cover steel plates. The dimension of the cover steel plates was 1000 mm by 1000 mm and 3 mm in thickness. Two types of core layers, rigid polyurethane foam (RPF) or vulcanized rubber (VR), were used. The behavior of these two types of lightweight sandwich panels was compared with the behavior of the hollow (H) core sandwich panel. Four core thicknesses (5, 10, 15 and 20 cm) were considered. The sandwich panels were then subjected to 1, 5 and 10 kg TNT explosion at a standoff distance of 1 m. The displacement time history is then measured at the center of the rear steel cover plate. Both of the RPF and VR core layers were modeled using Lagrange solid elements. A linear EOS and elastic strength model were used to model the behavior of the RPF material under explosion. Hyperelastic material EOS and strength model were used to describe the behavior of the rubber material against blast loads. Ogden model was used to describe the strength of rubber material as it can model the behaviour of rubber material up to 700% strain (Ansys 2007). Tables 6 and 7 show the mechanical properties of RPF and VR used in this study, respectively.

3. Assessment of the lightweight sandwich panels under different free air blast loads

A total of 36 numerical models were developed using Autodyn to simulate the dynamic response of the lightweight steel sandwich panels with different core materials. These numerical models illustrated the behavior

of hollow core sandwich panel (H), RPF core sandwich panel (RPF) and VR core sandwich panel (VR). A parametric study was applied by changing the core thickness of these lightweight sandwich panels and changing the explosion load value. The behavior of these different lightweight sandwich panels was compared to each other to show the effectiveness of adding RPF and VR.

Figs. 7-9 show the displacement time histories at the mid-span of the back panel of the hollow core sandwich panels subjected to 1, 5 and 10 kg TNT, respectively. Table 8 shows the ratios of maximum displacement at different

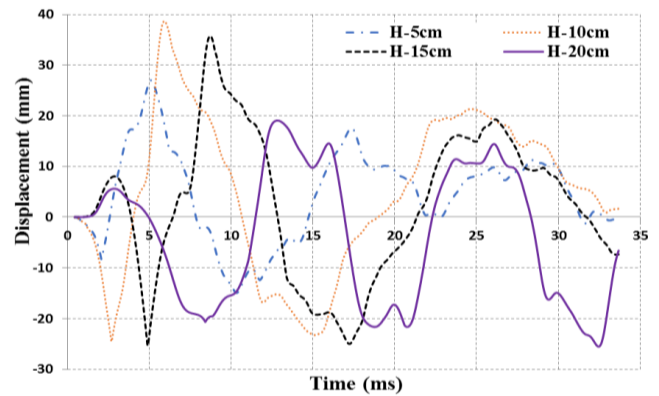


Fig. 7 Displacement time histories of Point 1 of H sandwich panels with thicknesses 5, 10, 15

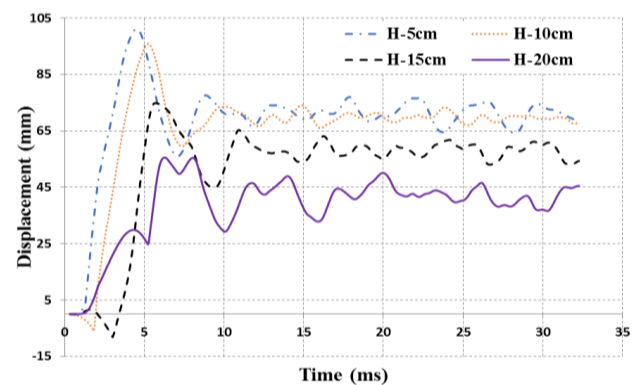


Fig. 8 Displacement time histories of Point 1 of H sandwich panels with thicknesses 5, 10, 15

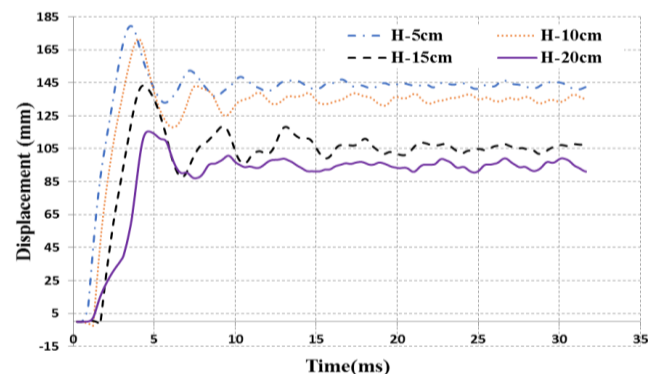


Fig. 9 Displacement time histories of Point 1 of H sandwich panels with thicknesses 5, 10, 15

Table 8 The ratios of maximum displacement values of RPF sandwich panels with different core thicknesses

Blast load values	H5 cm	H10 cm	H15 cm	H20 cm
1 kg TNT	--	--	--	--
5 kg TNT	1	0.96	0.75	0.56
10 kg TNT	1	0.96	0.80	0.65

core thicknesses and blast loads. As shown in Fig. 7, under 1 kg of TNT explosion, the residual deformation is zero. This shows that the steel sandwich panels remain elastic. It is noticed that there is suction occur in the hollow core sandwich panel. As the thickness of the hollow core increases, the maximum suction increases. For the 5 kg TNT (Fig. 8), all of the panels have residual displacement. This means the panel yielded. It is noticed that the suction decreases as the blast load increases from 1 kg of TNT to 5 kg of TNT. For the 10 kg TNT, the panels have the highest residual displacement. As the load increases from 5 kg of TNT to 10 kg of TNT, suction is approximately reached zero. A possible explanation for this suction is the effect of the wrapping pressure. As the blast wave wraps around the sandwich panel creating an opposite pressure in the rear plate of the sandwich panel. Wrapping pressure depends mainly on the velocity of the blast wave. Therefore,

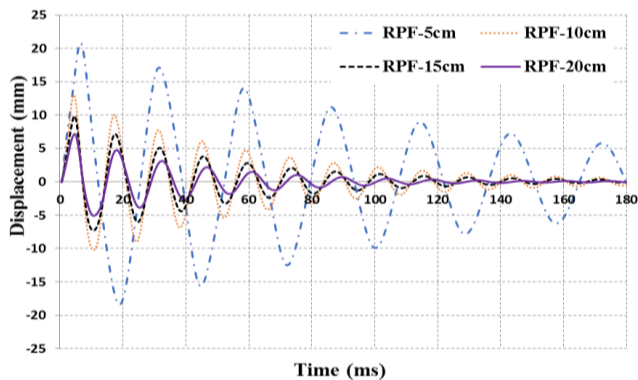


Fig. 10 Displacement time histories of Point 1 of RPF sandwich panels with thicknesses 5, 10, 15 and 20 cm subjected to 1 kg TNT at SOD of 1 m

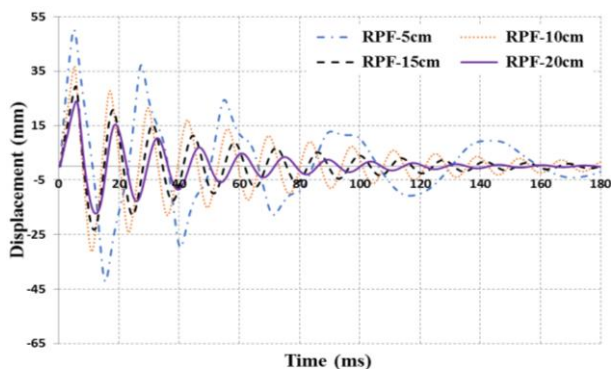


Fig. 11 Displacement time histories of Point 1 of RPF sandwich panels with thicknesses 5, 10, 15 and 20 cm subjected to 5 kg TNT at SOD of 1 m

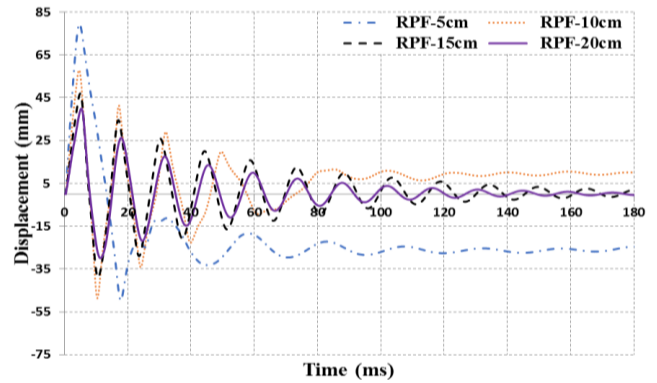


Fig. 12 Displacement time histories of Point 1 of RPF sandwich panels with thicknesses 5, 10, 15 and 20 cm subjected to 10 kg TNT at SOD of 1 m

Table 9 The ratio of maximum displacement values of RPF sandwich panels with different core thicknesses

Blast load values	RPF5 cm	RPF10 cm	RPF15 cm	RPF20 cm
1 kg TNT	1	0.62	0.47	0.34
5 kg TNT	1	0.73	0.58	0.48
10 kg TNT	1	0.73	0.59	0.50

wrapping pressure decreases with increasing blast loads.

Figs. 10-12 show the displacement time histories at the mid-span of the back panel of the RPF core sandwich panels subjected to 1, 5 and 10 kg of TNT denoted at SOD of 1 m, respectively. Table 9 shows the ratios of maximum displacement at different core thicknesses and blast loads. For the 1 kg TNT blast load, the residual deformation is zero. This shows that the panels remain elastic. For the 5 kg TNT blast load, the residual displacement for the RPF-20 cm, 15 cm and 10 cm are zero. But the residual displacement for the RPF-5 cm has a residual deflection of 4.3 mm. For the 10 kg TNT, only the RPF-20 cm and RPF-15 cm have zero residual displacements, while RPF-10 cm and RPF-5 cm have residual displacements of 9.0 mm, 26.6 mm, respectively.

Figs. 13-15 show the displacement time histories at the midpoint of the back plate of the VR core sandwich panels

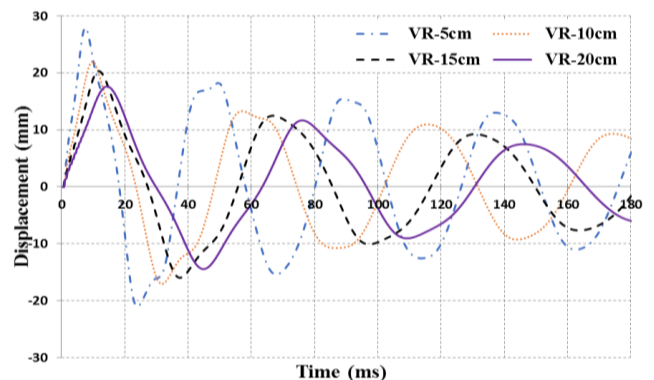


Fig. 13 Displacement time histories of Point 1 of VR sandwich panels with thicknesses 5, 10, 15 and 20 cm subjected to 1 kg TNT at SOD of 1 m

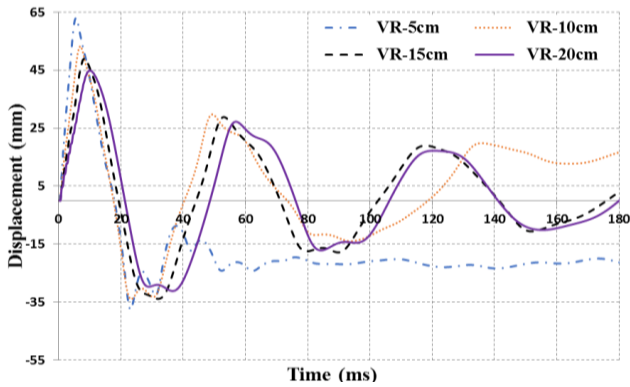


Fig. 14 Displacement time histories of Point 1 of VR sandwich panels with thicknesses 5, 10, 15 and 20 cm subjected to 5 kg TNT at SOD of 1 m

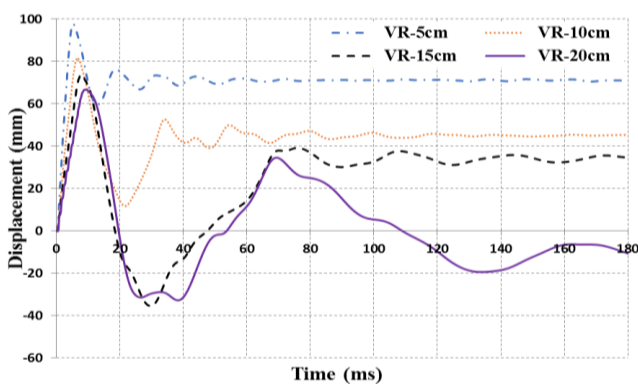


Fig. 15 Displacement time histories of Point 1 of VR sandwich panels with thicknesses 5, 10, 15 and 20 cm subjected to 10 kg TNT at SOD of 1 m

Table 10 The ratios of maximum displacement values of VR sandwich panels with different core thicknesses

Blast load values	RPF5 cm	RPF10 cm	RPF15 cm	RPF20 cm
1 kg TNT	1	0.79	0.73	0.63
5 kg TNT	1	0.85	0.78	0.71
10 kg TNT	1	0.83	0.75	0.68

subjected to 1, 5 and 10 kg TNT detonated at SOF of 1 m, respectively. Table 10 shows the ratios of maximum displacement at different core thicknesses and blast loads. For the 1 kg TNT loading case, the residual deformation returns to zero. This shows that the panels remain elastic. For 5 kg TNT loading case, the residual displacement VR-5 cm, VR-10 cm, VR-15 cm and VR-20 cm are of 21.8 mm, 14.7 mm, 5.5 mm, and 2.8 mm, respectively. For 10 kg TNT loading case, the residual displacement for the VR-5cm, VR-10 cm, VR-15 cm and VR-20 cm are 71.0 mm, 45.7 mm, 34.7 mm, and 12.3 mm, respectively.

It is noticed that the behavior of the RPF core sandwich panel outperformed that of VR core sandwich panel. The RPF sandwich panel behaves elastically for a good range of blast loads, while VR core sandwich panel goes to plastic deformation when the blast load exceeds 5 kg. Also, it is worth mentioning that the damping rate of RPF sandwich panel is greater than that of VR core sandwich panel. Fig. 16 illustrates the relationship between the maximum displacement values and the core thickness of RPF and VR sandwich panels for different blast load values of 1, 5 and 10 kg TNT. Table 11 shows the average reduction percentages of maximum displacement which occurred due to the replacement of VR with RPF as a core material of sandwich panels subjected to three different blast loads.

In order to facilitate the engineer to select the optimal core thickness for different blast loads, a simple empirical equation was derived using multiple regression to predict the maximum displacement of the steel sandwich panel with different core thickness and the blast loads. Overfitting and multicollinearity have been checked. It was found that each of the two independent variables (core thickness and charge weight) is highly correlated with the dependent variable (maximum displacement) but not between each other. Eqs. (3) and (4) show the empirical equations derived for steel

Table 11 The average reduction percentages of maximum displacement of RPF sandwich panels with different core thicknesses

Blast load values	1 kg TNT	5 kg TNT	10 kg TNT
Reduction percentages	59%	49%	40%

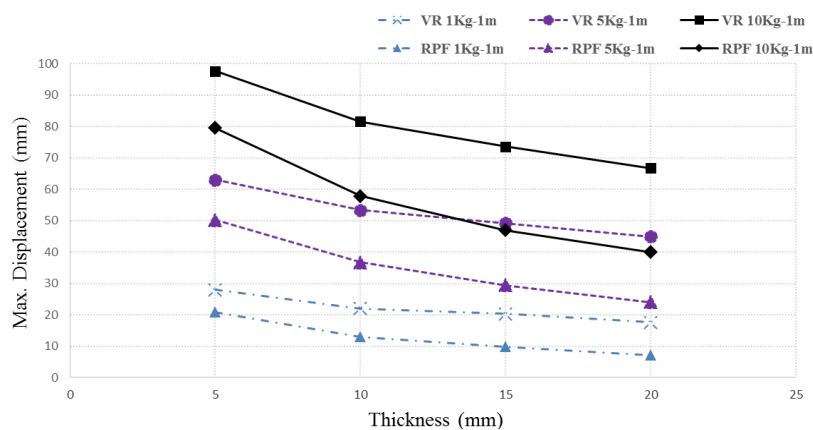


Fig. 16 Maximum displacement thickness chart of RPF and VR core sandwich panels with thicknesses 5, 10, 15 and 20 cm subjected to 1, 5 and 10 kg TNT at SOD of 1 m

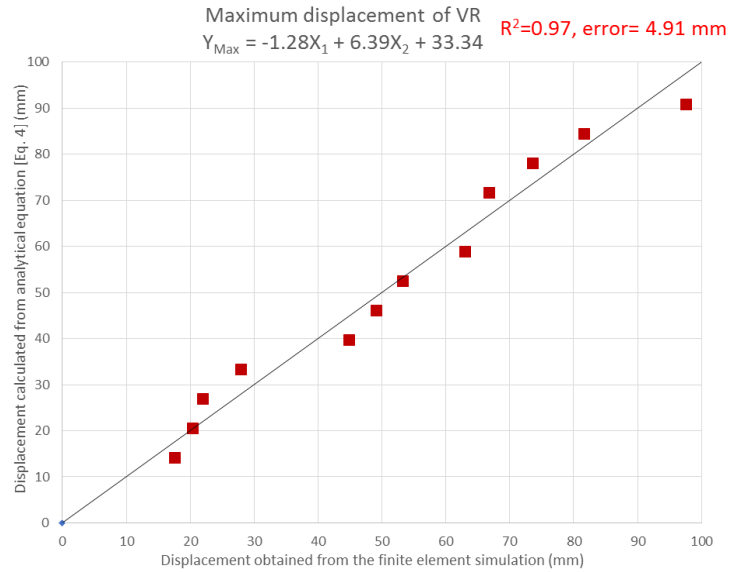


Fig. 20 Comparing the maximum displacement of VR sandwich panel calculated using finite element simulation and the empirical equation shown in Eq. (3)

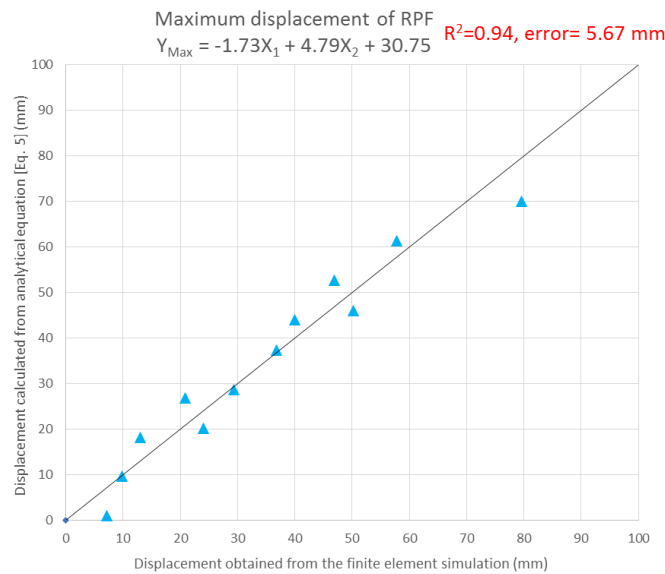


Fig. 21 Comparing the maximum displacement of RPF sandwich panel calculated using finite element simulation and the empirical equation shown in Eq. (4)

sandwich core with VR and RPF core, respectively. The results of the empirical equation were plotted against the results of the finite element simulation and shown in Figs. 20 and 21. The result shows the empirical equation presented in Eqs. (3) and (4) can be reliably used to estimate the maximum displacement of the steel sandwich panels with different thickness and blast loads. The empirical equation can match the finite element results well with standard deviation error within 5 and 6 mm for the VR and RPF core, respectively.

$$Y_{max} = -1.28X_1 + 6.39X_2 + 33.34 \dots \dots \dots \text{For VR} \quad (3)$$

$$Y_{max} = -1.73X_1 + 4.79X_2 + 30.754 \dots \dots \dots \text{For RPF} \quad (4)$$

Where: X_1 is the thickness of the core layer in (mm), X_2

is the TNT weight in (Kg) and Y_{max} is the maximum displacement at the center of the sandwich panel in (mm).

4. Conclusions

Steel sandwich panels have been used as efficient structural components to resist blast loads. However, the steel only sandwich panels are heavy. To decrease the weight of these protective steel sandwich panels, novel steel sandwich panels with different lightweight core materials were investigated. To simulate the dynamic response of these steel sandwich panels, under different blast loads, advanced finite element models of these sandwich panels were developed in Autodyn. The finite element models were verified against experimental results. Detailed

parameter study, with different lightweight core materials and different core thickness under a different range of TNT explosion loads, were investigated. The following conclusions were made:

- The proposed finite element approach was validated against experimental data and the commonly used blast engineering software CONWEP. The results show the proposed model can be used reliably to model the nonlinear behaviour of the steel sandwich panel under different blast loads.
- The lightweight sandwich panel with RPF and VR core material can reduce the weight of the steel only sandwich panel and with improved dynamic responses.
- Using VR as a core layer can reduce the maximum displacement of the hollow steel sandwich panel by an average of 42%.
- Using RPF as a core layer can reduce the maximum displacement of the hollow steel sandwich panel by an average of 53% and can reduce the maximum displacement by an average of 49% when replacing VR core layer.
- The proposed empirical equations developed matched the maximum deformation of the panels under different blast loads with different core materials. This means the simple proposed empirical equations can be used by engineers to select the different thickness of sandwich panel core material (RPF and VR) for different blast load applications.

Acknowledgments

The authors are grateful to the financial support by the Egyptian army and Also, for the manufactural assistance and the technical information provided by Military Technical College (MTC).

References

- Ansys (2007), Theory reference manual; Release 11.0, Ansys Inc.
- Chen, Y., Tong, Z.P., Hua, H.X., Wang, Y. and Gou, H.Y. (2009), "Experimental investigation on the dynamic response of scaled ship model with rubber sandwich coatings subjected to underwater explosion", *Int. J. Impact Eng.*, **36**(2), 318-328.
- Fayad, H.M. (2009), "The optimum design of the tunnels armoured doors under blast effects", Ph.D. Dissertation; Military Technical College (MTC), Cairo, Egypt.
- Ha, J., Yi, N., Choi, J. and Kim, J. (2011), "Experimental study on hybrid CFRP-PU strengthening effect on RC panels under blast loading", *J. Compos. Struct.*, **93**, 2070-2082.
- Hyde, D.W. (1991), "CONWEP-Conventional Weapons Effects Program", US Army Waterways Experiment Station; Vicksburg, MS, USA.
- Johnson, G.R. and Cook, W.H. (1983), "A constitutive model and data for metals subjected to large strains, high strain rates and high temperatures", *Proceedings of the 7th International Symposium on Ballistics*, The Hague, The Netherlands, pp. 541-547.
- Lee, D.K. (David) and O'Toole, B.J. (2004), "Energy absorbing sandwich structures under blast loading", Doctoral Dissertation; *Proceedings of the 8th International LS-DYNA User Conference*, **8**, p. 13-24.
- Li, X., Miao, C., Wang, Q. and Geng, Z. (2016), "Antiknock performance of interlayered high-damping-rubber blast door under thermobaric shock wave", *Shock Vib.*, Article ID 2420893, 9 pages.
- Mazek, S.A. (2014), "Performance of sandwich structure strengthened by pyramid cover under blast effect", *Struct. Eng. Mech., Int. J.*, **50**(4), 471-486.
- Mazek, S. and Mostafa, A. (2013), "Impact of a shock wave on a structure strengthened by rigid polyurethane foam", *J. Struct. Eng. Mech., Int. J.*, **48**(4), 569-585.
- Mazek, S.A. and Mostafa, A.A. (2014), "Impact of composite materials on performance of reinforced concrete panels", *Comput. Concrete, Int. J.*, **14**(6), 767-783.
- Mazek, S.A. and Wahab, M.A. (2015), "Impact of composite materials on buried structures performance against blast wave", *J. Struct. Eng. Mech.*, **53**(3), 589-605.
- Mostafa, A.A., Salem, A.H., Wahab, M.A. and Mazek, S.A. (2010a), "Blast mitigation using polyurethane foam to retrofit fortified sandwich structures", *Proceedings of the 8th International Conference on Civil and Architecture Engineering ICCAE*, Cairo, Egypt, May.
- Mostafa, H.E., El-Dakhkhni, W.W. and Mekky, W.F. (2010b), "Use of reinforced rigid polyurethane foam for blast hazard mitigation", *J. Reinf. Plast. Compos.*, **29**(20), 3048-3057.
- Nurick, G.N., Langdon, G.S., Chi, Y. and Jacob, N. (2009), "Behaviour of sandwich panels subjected to intense air blast - Part 1: Experiments", *Compos. Struct.*, **91**(2009), 433-441.
- Rashad, M. (2013), "Study the Behavior of Composite Sandwich Structural Panels under Explosion Using Finite Element Method", M.Sc. Thesis; Military Technical College (MTC), Cairo, Egypt.
- Sheikh, S.A. and Li, Y. (2007), "Design of FRP confinement for square concrete columns", *Eng. Struct.*, **29**(6), 1074-1083.
- TM 5-885-1 (1986), *Fundamentals of Protective Design for Conventional Weapons*; Headquarters Department of the Army, Washington, DC, USA.
- Vinson, J.R. (2001), "Sandwich structures", *Appl. Mech. Rev.*, **54**(3), 201-214
- Wang, Y.C. and Ko, C.C. (2015), "Energy dissipation of steel-polymer composite beam-column connector", *Steel Compos. Struct., Int. J.*, **18**(5), 1161-1176.
- Woodfin, R.L. (2000), "Using Rigid Polyurethane Foams (RPF) for Explosive Blast Energy Absorption in Applications Such as Anti-Terrorist Defenses", Research Report; No. SAND2000-0958, Sandia National Laboratories, CA, USA.
- Woodfin, R.L., Faucett, D.L., Hance, B.G., Latham, A.E. and Schmidt, C.O. (1998), "Results of Experiments on Rigid Polyurethane Foam (RPF) for Protection from Mines", Research Report; No. SAND98-2278, Sandia National Laboratories, CA, USA.
- Xia, Z., Wang, X., Fan, H., Li, Y. and Jin, F. (2016), "Blast resistance of metallic tube-core sandwich panels", *Int. J. Impact Eng.*, **97**, 10-28.
- Xiao, F., Chen, Y. and Hua, H. (2014), "Comparative study of the shock resistance of rubber protective coatings subjected to underwater explosion", *J. Offshore Mech. Arct. Eng.*, **136**(2), 021402-021402-12. DOI: 10.1115/1.4026670
- Yen, C.F., Skaggs, R. and Cheeseman, B.A. (2005), "Modeling of shock mitigation sandwich structures for blast protection", *Proceedings of the 3rd International Conference on Structural Stability and Dynamics*, FL, USA, June.
- Zhu, F. (2008), "Impulsive loading of sandwich panels with cellular cores", Ph.D. Dissertation; Swinburne University of Technology, Hawthorn, Melbourne, VIC, Australia.